Study of the Burning Rates of Aluminized Composite Propellants in Acceleration Fields," AIAA Paper 68-529, Atlantic City, N.J., June 1968.

[7] Northam, G. B. and Lucy, M. H., "On the Effects of Acceleration Upon Solid Rocket Performance," presented at the Third ICRPG/AIAA Solid Propulsion Conference, Atlantic City, N.J., June 1968.

[8] Willoughby, P. G., Baker, K. L., and Crowe, C. T., "A Photographic and Analytic Study of Composite Propellant Combustion in an Acceleration Field," AIAA Paper 69-173, New York, 1969.

[9] Mager, A., "Approximate Solution of Isentropic Swirling Flow Through a Nozzle," *ARS Journal*, Vol. 31, No. 8, Aug. 1961, pp. 1140–1148.

[10] Norton, D. J., Farquhar, B. W., and Hoffman, J. D., "An Analytical and Experimental Investigation of Swirling Flow in Nozzles," F-67-9, Oct. 1697, Jet Propulsion Center, Purdue Univ., Lafayette, Ind.

[11] Küchemann, D., *Progress in Aeronautical Sciences, Volume 7*, 1st ed., Pergamon Press, Oxford, 1966.

[12] Long, R. R., "Sources and Sinks at the Axis of a Rotating Liquid," *Quarterly Journal of Mechanics and Applied Mathematics*, Vol. IX, Pt. 4, 1956, pp. 385–393.

[13] Batchelor, G. K., *An Introduction to Fluid Dynamics*, Cambridge Univ. Press, 1967.

[14] Johnson, G. R. and L'Ecuyer, M. R., "An Experimental Investigation of the Pressure and Velocity Profiles in a Spinning, Cold-Flow Rocket Motor," TM-68-6, August 1968, Jet Propulsion Center, Purdue Univ., Lafayette, Ind.

DECEMBER 1969 AIAA JOURNAL VOL. 7, NO. 12

Onset of Instabilities in Coaxial Hall Current Accelerators

H. A. HASSAN* AND CHARLES C. THOMPSON†
North Carolina State University, Raleigh, N.C.

An analysis is presented with the objective of predicting the onset of spokes in MPD arcs. A simple geometry consisting of coaxial electrodes with applied radial electric field and axial magnetic field is investigated with the analysis being based upon the ion and electron conservation equations. After obtaining a steady-state solution that takes into consideration the existence of anode and cathode sheaths, an $m = 1$ helical perturbation is analyzed using a normal mode analysis. The results indicate that the critical magnetic field increases with pressure, and because of the geometry chosen, it is independent of the current. The instability is of the Simon-Hoh type.

Introduction

EXPERIMENTS at various laboratories[1–4] indicate that, under certain operating conditions, the arc current in an MPD thruster tends to concentrate into a rotating spoke. This form of instability rotates in the $\mathbf{E} \times \mathbf{B}$ direction with an angular velocity that increases with magnetic field strength and current but decreases with mass flow rate. More recent experiments[5,6] indicate that the formation of the spoke is associated with an onset with the critical magnetic field being of the order of a few hundred gauss.

The object of this investigation is to determine the onset of instabilities in MPD arcs. The usual procedure employed in studies of this nature is to obtain a steady-state solution of the governing equations that are assumed to be the conservation equations for the ions and electrons. A perturbation is then superimposed on the system; if it does not grow with time the system is stable, otherwise it is unstable. There are at least two major complications associated with such a procedure for the problem under consideration. The complexity of the geometry makes it impossible to obtain an analytical solution. In addition, even when a simple geometry is assumed, one cannot ignore the anode and cathode sheaths as is normally done in the study of similar problems for the positive column,[7] or the linear Hall current accelerator.[8]

In this work, a simple geometry consisting of an inner cathode and an outer ring anode combined with an axial magnetic field (Fig. 1) is employed. The electric and magnetic field arrangement considered here is similar to that discussed by Hoh[9] for a Penning discharge. The analysis presented here differs from that of Ref. 9 in that a steady-state solution that takes into consideration the existence of anode and cathode sheaths has been obtained, and a normal mode analysis instead of dimensional analysis is used to analyze the instability.

The governing equations are the usual conservation of mass and momentum for ions and electrons. The inertia terms in the ion and electron momentum equations are usually ignored and this assumption has been made here. Although one is justified in ignoring the electron inertia terms, neglect of the ion inertia terms requires further justification. A partial justification follows from the work of Persson[10] on the positive column where it is shown that linear ambipolar diffusion gives a fairly good approximation of the steady-state solution if the ambipolar velocity is less than the speed of sound of the ion-electron pair. This, coupled with the fact that for the problem under consideration, the radial ion current is much less than the radial electron current, indicates that neglecting the ion inertia terms is justified provided one uses appropriate boundary conditions.

Using a procedure similar to that employed for the positive column, the appropriate boundary conditions at the edge of the cathode sheath can be inferred from investigation of the singular points of the complete differential equations. As is shown in Appendix A, the limiting velocity at the edge of the cathode sheath reduces to the speed of sound of the ion-electron pair when the net current is zero. The boundary condition at the edge of the anode sheath is obtained from the consideration that the current density is approximately equal to the random electron current density.

The steady-state solution obtained shows that the product of the radial component of the electric field and the density

Presented as Paper 69-230 at the AIAA 7th Electric Propulsion Conference, Williamsburg, Va., March 3–5, 1969; submitted February 19, 1969; revision received June 30, 1969. This work was supported, in part, by NASA Grant NGR 34-002-048.

* Professor of Mechanical and Aerospace Engineering. Associate Fellow AIAA.

† Research Assistant.

gradient in its direction is positive. It may be recalled that the aforementioned is a necessary condition for instabilities in devices employing crossed electric and magnetic fields.[11] The driving mechanism is that discussed by Hoh[9] where the electric field resulting from charge separation, and the density gradient combine to amplify the perturbation.

Analysis

A. Governing Equations

The governing equations are the conservation equations of mass and momentum for a slightly ionized gas in the presence of electric and magnetic fields

$$\partial n_s/\partial t + \nabla\cdot(n_s\mathbf{V}_s) = n_e\xi \tag{1}$$

$$q_s n_s(\mathbf{E} + \mathbf{V}_s \times \mathbf{B}) - KT_s\nabla n_s - n_s\nu_s\mathbf{V}_s = 0,\ s = i,e \tag{2}$$

where n is the number density, q the charge, $\mathbf{E}$ and $\mathbf{B}$ the electric and magnetic fields, respectively, $\mathbf{V}$ the particle velocity, T the temperature, K the Boltzmann constant, m the particle mass, ν the collision frequency with the neutrals, ξ the number of ionizing collisions per electron per second, and the subscripts i and e refer to ions and electrons respectively. In writing Eq. (2), it has been assumed that the inertia terms are negligible and that the temperatures are constant. Equation (2) can be solved explicitly for the particle flux and the result can be written as

$$\begin{aligned}\mathbf{\Gamma}_{i,e} = n_{i,e}\mathbf{V}_{i,e} = {}& \pm\mu'_{i,e}n_{i,e}\mathbf{E} - D'_{i,e}\nabla n_{i,e} \mp \\ & \mu_{i,e}D'_{i,e}\nabla n_{i,e}\times\mathbf{B} \pm \mu_{i,e}{}^2\mu'_{i,e}n_{i,e}(\mathbf{E}\cdot\mathbf{B})\mathbf{B} - \\ & \mu_{i,e}{}^2 D_{i,e}(\nabla n_{i,e}\cdot\mathbf{B})\mathbf{B} + \mu_{i,e}\mu'_{i,e}n_{i,e}\mathbf{E}\times\mathbf{B}\end{aligned} \tag{3}$$

where

$$\begin{aligned}\mu_s = e/m_s\nu_s,\ D_s = KT_s/m_s\nu_s,\ \mu'_s = \mu_s/(1 + \mu_s{}^2B^2) \\ D'_s = D_s/(1 + \mu_s{}^2B^2),\ e = |q_s|\end{aligned} \tag{4}$$

In the bulk of the plasma $n_i \approx n_e$. Combining Eqs. (1) and (3) and letting $n_i \approx n_e = n$, one obtains

$$\begin{aligned}\partial n/\partial t - n\xi \pm \mu'_{i,e}\nabla\cdot(n\mathbf{E}) - D'_{i,e}\nabla^2 n \mp \\ \mu_{i,e}D'_{i,e}\nabla\cdot(\nabla n \times \mathbf{B}) \pm \mu_{i,e}{}^2\mu'_{i,e}\nabla\cdot(n\mathbf{E}\cdot\mathbf{B})\mathbf{B} - \\ \mu_{i,e}{}^2D'_{i,e}\nabla\cdot(\nabla n\cdot\mathbf{B})\mathbf{B} + \mu_{i,e}\mu'_{i,e}\nabla\cdot(n\mathbf{E}\times\mathbf{B}) = 0\end{aligned} \tag{5}$$

In deriving Eq. (5) it is assumed that any induced magnetic fields are much smaller than the externally applied constant field. Equation (5) forms the basis of the stability analysis. A steady-state solution is first obtained and then the resulting solution is perturbed. Thus, letting

$$n = n_0 + n_1,\ \mathbf{E} = \mathbf{E}_0 + \mathbf{E}_1 \tag{6}$$

where n_0 and $\mathbf{E}_0$ represent the steady-state solution, substituting into Eq. (5) and ignoring higher-order terms, one finds

$$\begin{aligned}\partial n_1/\partial t - n_1\xi \pm \mu'_{i,e}\nabla\cdot(n_0\mathbf{E}_1 + n_1\mathbf{E}_0) - D'_{i,e}\nabla^2 n_1 \mp \\ \mu_{i,e}D'_{i,e}\nabla\cdot(\nabla n_1 \times \mathbf{B}) \pm \mu_{i,e}{}^2\mu'_{i,e}\nabla\cdot\{[B\cdot(n_0\mathbf{E}_1 + \\ n_1\mathbf{E}_0)]\mathbf{B}\} - \mu_{i,e}{}^2D'_{i,e}\nabla\cdot[(\nabla n_1\cdot\mathbf{B})\mathbf{B}] + \\ \mu_{i,e}\mu'_{i,e}\nabla\cdot[(n_0\mathbf{E}_1 + n_1\mathbf{E}_0)\times\mathbf{B}] = 0\end{aligned} \tag{7}$$

A normal mode analysis is used to obtain the dispersion relation from Eq. (7) and, hence, the conditions for instability.

B. Steady-State Solution

For the coaxial geometry under consideration all the properties are functions of the radial coordinate r. Thus, Eq. (1) reduces to

$$(1/r)(d/dr)[rn_0(V_{i,r} - V_{e,r})] = 0$$

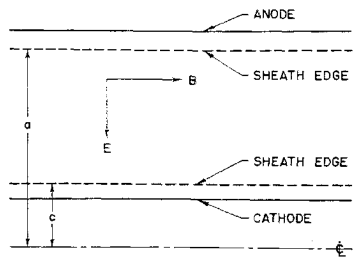

Fig. 1 Schematic of a coaxial Hall current accelerator.

or

$$-j = 2\pi re[\Gamma_{i,r} - \Gamma_{e,r}] \tag{8}$$

where j is the current per unit length. The expressions for $\Gamma_{i,r}$ and $\Gamma_{e,r}$ follow from Eq. (3) as

$$\begin{aligned}\Gamma_{i,r} &= \mu'_i n_0 E_{o,r} - D'_i\partial n_0/\partial r \\ \Gamma_{e,r} &= -\mu'_e n_0 E_{o,r} - D'_e\partial n_0/\partial r\end{aligned} \tag{9}$$

Substituting Eqs. (9) into Eq. (8), one finds

$$E_{o,r} = -\frac{(j/2\pi er) + (D'_e - D'_i)(\partial n_0/\partial r)}{n_0(\mu'_i + \mu'_e)} \tag{10}$$

thus, the ion and electron fluxes reduce to

$$\Gamma_{i,r} = -\frac{\mu'_i j}{2\pi re(\mu'_i + \mu'_e)} - \frac{a^2\xi}{\beta_0{}^2}\frac{\partial n_0}{\partial r} \tag{11}$$

$$\Gamma_{e,r} = \frac{\mu'_e j}{2\pi re(\mu'_i + \mu'_e)} - \frac{a^2\xi}{\beta_0{}^2}\frac{\partial n_0}{\partial r} \tag{12}$$

where

$$\beta_0{}^2 = a^2\xi(\mu'_i + \mu'_e)/(\mu'_i D'_e + \mu'_e D'_i) \tag{13}$$

and a is the radius of anode sheath. The governing equation for the steady-state density distribution follows from Eqs. (1) and (11) as

$$(1/r)(d/dr)(rdn_0/dr) + (\beta_0{}^2/a^2)n_0 = 0 \tag{14}$$

which gives

$$n_0 = (j/2\pi e)[C_1J_0(\beta_0 r/a) + C_2Y_0(\beta_0 r/a)] \tag{15}$$

Expressions for C_1 and C_2 are obtained from the boundary conditions. As is seen from Appendix A, the appropriate boundary condition at the edge of the cathode sheath, $r = c$, is

$$V_{i,r} = -[1/(1 + \mu)]\{j/2\pi cen + [\mu(1 + \mu)u_0{}^2 - \mu(j/2\pi cen)^2]^{1/2}\}$$

where

$$u_0{}^2 = K(T_i + T_e)/m_i,\ \mu = m_i/m_e \tag{16}$$

Assuming that the thickness of the anode sheath is less than a heavy particle mean free path, the desired boundary condition may be obtained from requiring that the current density be equal to the free molecule expression at the sheath edge, or

$$j_r = \tfrac{1}{4}[en_ec_e - en_ic_i\exp(-\phi/KT_i)] \tag{17}$$

where ϕ is the potential drop across the anode sheath. Because

$$c_s = (8K\ T_s/\pi m_s)^{1/2} \tag{18}$$

Eq. (17) gives

$$V_{e,r} \approx (KT_e/2\pi m_e)^{1/2} \text{ at } r = a \tag{19}$$

The desired expressions for C_1 and C_2 follow from Eqs. (11, 12, 15, 16, and 19); it is to be noted that both C_1 and C_2 are independent of j. Both the number density and electric field, which depend on the applied magnetic field, remain

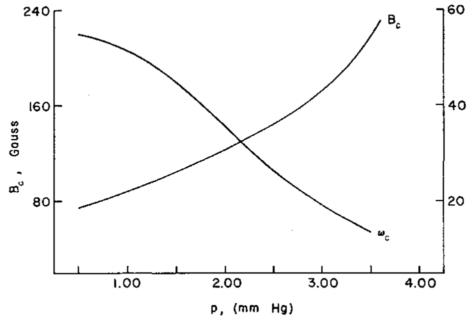

Fig. 2 Critical magnetic field and frequency vs pressure.

finite throughout. It is seen from Eqs. (10) and (15) that the radial electric field is independent of the current and hence a voltage plateau exists. This indicates that, for the preceding steady-state solution, the onset of instability is independent of the current.

C. Normal Mode Analysis

In order to study the stability of the steady-state solution, the perturbations n_1 and $\mathbf{E}_1$ will be chosen as

$$n_1 = f(r)\exp[i(\omega t + m\theta + kx)]$$
$$\mathbf{E} = -\nabla U, U = g(r)\exp[i(\omega t + m\theta + kx)] \tag{20}$$

with m and k real and ω complex. Substituting Eq. (2) into Eq. (7), one obtains

$$D'_{i,e}\left[\frac{1}{r}\frac{d}{dr}\left(r\frac{df}{dr}\right) - \frac{m^2}{r^2}f\right] + \left[\xi - i\omega - D_{i,e}k^2 + \mu_{i,e}\mu'_{i,e}\frac{imB}{r}E_{o,r}\right]f \mp \frac{\mu'_{i,e}}{r}\frac{d}{dr}(rfE_{o,r}) = \mp\mu'_{i,e}\left[\frac{1}{r}\frac{d}{dr}\left(rn_0\frac{dg}{dr}\right) - \frac{m^2}{r^2}n_0g\right] \pm \mu_{i,e}k^2n_0g - \mu_{i,e}\mu'_{i,e}\frac{imB}{r}\frac{dn_0}{dr}g \tag{21}$$

Letting

$$n_0g = h(r) + [(D'_e - D'_i)/(\mu'_i + \mu'_e)]f(r)$$
$$\omega_0 = \omega/\xi,\ k_0 = ka,\ R = r/a,\ n_0 = (j/2\pi e)N_0 \tag{22}$$

using Eq. (10) to eliminate $E_{o,r}$ and noting that

$$D'_{i,e} \pm (D'_e - D'_i)/(\mu'_i + \mu'_e) = \xi a^2/\beta_0^2 \tag{23}$$

Eq. (21) reduces to

$$\frac{\xi}{\beta_0^2}\left[\frac{1}{R}\frac{d}{dR}\left(R\frac{df}{dR}\right) - \frac{m^2}{R^2}f\right] + \xi\left[1 - i\omega_0 - \frac{k_0^2}{\beta_0^2}(1 + \mu_{i,e}^2B^2)\right]f \pm \frac{\mu'_{i,e}}{a^2(\mu'_i + \mu'_e)}\left[\mp imB\frac{\mu_{i,e}f}{R^2N_0} + \frac{1}{R}\frac{d}{dR}\left(\frac{f}{N_0}\right)\right] = \pm\frac{\mu'_{i,e}}{a^2}\left\{-\left[\frac{1}{R}\frac{d}{dR}\left(R\frac{dh}{dR}\right) - \frac{m^2}{R^2}h\right] + k_0^2(1 + \mu_{i,e}^2B^2)h \mp \mu_{i,e}\frac{imB}{R} \times \frac{h}{N_0}\frac{dN_0}{dR} + \frac{1}{R}\frac{d}{dR}\left(R\frac{h}{N_0}\frac{dN_0}{dR}\right)\right\} \tag{24}$$

Equation (24) does not have a closed form solution and, therefore, transform techniques will be employed to derive the dispersion relation. The general dispersion relation is derived in Appendix B. Because of its complexity, an approximate form of this relation will be obtained by assuming the forms of $f(R)$ and $h(R)$. Thus, if one lets

$$f(R) = A_1G_m(\delta_1R),\ h(R) = A_2G_m(\delta_1R), A_1, A_2 = \text{const} \tag{25}$$

where

$$G_m(\delta_1R) = Y_m(\delta_1R)J_m(\delta_1c/a) - J_m(\delta_1R)Y_m(\delta_1c/a)$$
$$G_m(\delta_1) = 0 \tag{26}$$

then, multiplication of Eq. (24) by $RG_m(\delta_1R)$, integration between c/a and 1, and elimination of A_1 and A_2 yields the approximate dispersion relation. A partial justification of this procedure is given in Appendix B. Letting

$$\omega_0 = \omega_1 + i\omega_2 \tag{27}$$

the approximate dispersion relation can be written as

$$[\omega_2 + \sigma_{1i} + i(\lambda_{1i} - \omega_1)][\sigma_{2e} + i\lambda_{2e}] + [\omega_2 + \sigma_{1e} + i(\lambda_{1e} - \omega_1)][\sigma_{2i} + i\lambda_{2i}] = 0 \tag{28}$$

where

$$\sigma_{1i,e} = 1 - \frac{\delta_1^2}{\beta_0^2} - \frac{k_0^2}{\beta_0^2}(1 + \mu_{i,e}^2B^2) \pm \frac{\mu'_{i,e}}{\xi(\mu'_i + \mu'_e)a^2}\cdot(ma_{11} - \delta_1b_{11})$$
$$\sigma_{2i,e} = \mp\mu'_{i,e}[\delta_1^2 + (1 + \mu_{i,e}^2B^2)k_0^2 + mc_{11} - \delta_1d_{11}] \tag{29}$$
$$\lambda_{1i,e} = -\frac{m\mu_{i,e}\mu'_{i,e}}{\xi(\mu'_i + \mu'_e)a^2}Ba_{11}, \lambda_{2i,e} = m\mu_{i,e}\mu'_{i,e}Bc_{11}$$

The quantities a_{11}, b_{11}, c_{11}, and d_{11} are defined in Appendix B.

Expressions for ω_1 and ω_2 can be obtained from Eq. (28) by setting the real and imaginary parts equal to zero. For stability $\omega_2 \geq 0$, or from Eq. (28),

$$(\sigma_{2e} - \sigma_{2i})(\sigma_{1e}\sigma_{2i} - \sigma_{1i}\sigma_{2e}) + (\lambda_{2e} - \lambda_{2i}) \times (\sigma_{1e}\lambda_{2i} - \sigma_{1i}\lambda_{2e}) + (\lambda_{1e} - \lambda_{1i})(\sigma_{2i}\lambda_{2e} - \sigma_{2e}\lambda_{2i}) \geq 0 \tag{30}$$

while the frequency is given by

$$\omega_1 = [(\sigma_{1i} - \sigma_{2e})(\lambda_{2i}\sigma_{2e} - \lambda_{2e}\sigma_{2i}) + (\sigma_{2i} - \sigma_{2e}) \times (\lambda_{1e}\sigma_{2i} - \lambda_{1i}\sigma_{2e}) + (\lambda_{2e} - \lambda_{2i})(\lambda_{1i}\lambda_{2e} - \lambda_{1e}\lambda_{2i})][(\sigma_{2e} - \sigma_{2i})^2 + (\lambda_{2e} - \lambda_{2i})^2]^{-1} \tag{31}$$

As an application of the preceding analysis, the case of a helical perturbation, $m = 1$, in argon is considered. In this case, the collision frequencies and the ionization frequency can be written as[12]

$$\nu_e = \tfrac{2}{3}(2KT_e/m_e)^{1/2}(P/KT_i)Z_{ea}$$
$$\nu_i = \tfrac{2}{3}(KT_i/m_i)^{1/2}(P/KT_i)Z_{ia}$$
$$\xi = \frac{2}{(\pi)^{1/2}}\frac{P}{KT_i}m_ea_{ea}\left(\frac{I}{m_e}\right)^{3/2}\left(\frac{2KT_e}{I}\right)^{1/2} \times \left(1 + \frac{2KT_e}{I}\right)\exp\left(-\frac{I}{KT_e}\right)$$
$$Z_{ea} = 1.64706 \times 10^{-19} + 1.25947 \times 10^{-19}[T_e/10^4 - 1.27655],\ \text{m}^2$$
$$Z_{ia} = 1.6383 \times 10^{-18}\left\{1 - \left[\ln\left(\frac{T_i}{23{,}210}\right)\right] \times \left[0.1302 - 0.648 \times 10^{-2}\ln\left(\frac{T_i}{23{,}210}\right)\right]\right\},\ \text{m}^2$$
$$a_{ea} = 4.375 \times 10^{-3}\ \text{m}^2/\text{joule} \tag{32}$$

with I being the ionization potential. Thus, for a given pressure and temperatures, Eq. (30) represents a relation between k_0 and B. At the stability boundary, $\omega_2 = \partial\omega_2/\partial k_0 = 0$; these two conditions give B_c and $k_{0,c}$, the critical magnetic field and the critical wave number, respectively.

The frequency at the stability boundary is obtained from Eq. (31) by setting $B = B_c$ and $k_0 = k_{0,c}$.

Results and Discussion

The results shown in Figs. 2–4 are for $T_e = 20{,}000°K$, $T_i = 3{,}000°K$, and $a = 1.27$ cm. Figure 2 shows a plot of the critical magnetic field and frequency at the stability boundary vs pressure. The trends indicated in the plot are in agreement with the measurements of Ref. 5 for the linear Hall current accelerator. Although some preliminary measurements are reported in Ref. 5 for the MPD arc, direct comparison of this theory with these measurements is not possible because the pressures at which the experiment was carried out were not reported. Figure 3 shows that the critical magnetic field is practically independent of c/a. Thus, for a given a, uncertainties in the value of c do not have much influence on the onset of instabilities. As is seen from Fig. 4, the wave length, $\lambda = 2\pi/k_{0,c}$, increases with pressure.

In order to check the predictions of the theory, detailed measurements in the MPD arc, similar to those presented in Ref. 5 for the linear Hall accelerator, are needed. The theory presented here predicts an onset which is independent of the current. Based on the measurements of Ref. 6, it appears that this theory is applicable in the "weak B regime" where the current has little or no influence on the onset.

For higher B fields, the available measurements suggest that the critical magnetic field depends on the current. The reason for this discrepancy between theory and experiment can be traced to the geometry and to the fact that the nonlinear inertia terms in the momentum equations were assumed negligible. For the coaxial geometry selected here, axial currents cannot be allowed and the number density is proportional to the current. On the other hand, when the complete equations are employed, or when three dimensional effects are taken into consideration, the steady state solution will depend on the current in a nonlinear way. In such a case the critical magnetic field will depend on the current.

Appendix A: Boundary Conditions at the Edge of the Cathode Sheath

Assuming that all properties are function of r only, the conservation equations of mass and momentum for ions and electrons can be written as

$$(d/dr)(n_sV_{s,r}) = -n_sV_{s,r}/r + \xi n_e \tag{A1}$$

$$n_sV_{s,r}\frac{dV_{s,r}}{dr} + \frac{kT_s}{m_s}\frac{dn_s}{dr} = n_s\frac{V_{s,r}{}^2}{r} + \frac{n_sq_s}{m_s}\times (E_r + V_{s,\theta}B) - n_s\nu_sV_{s,r} \tag{A2}$$

$$V_{s,r}\frac{dV_{s,\theta}}{dr} + \frac{V_{s,r}V_{s,\theta}}{r} = -\frac{q_s}{m_s}V_{s,r}B - \nu_sV_{s,\theta} \tag{A3}$$

Equations (A1) and (A2) may be solved for dn_s/dr and $dV_{s,r}/dr$. Making use of the assumption that $n_i = n_e = n$ and setting $dn_i/dr = dn_e/dr$ yields an expression for E_r. Eliminating E_r from the expression for dn/dr, one finds

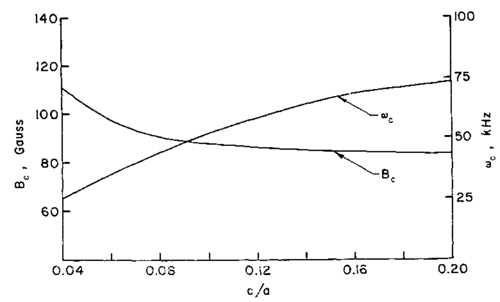

Fig. 3 Influence of effective electrodes radii on the critical magnetic field and frequency.

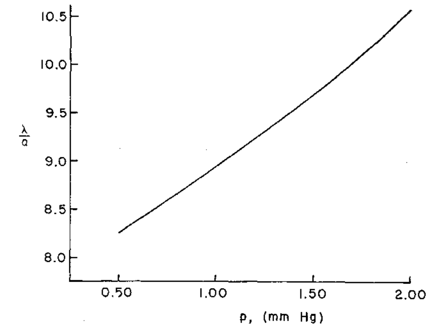

Fig. 4 Effect of pressure on wave length.

$$\frac{1}{n}\frac{dn}{dr} = -\frac{2}{r} + \frac{1}{\mu[u_0{}^2 - V_{i,r}{}^2] - V_{e,r}{}^2}\times \left\{\mu\left[-(\xi+\nu_i)V_{i,r} + \frac{eB}{m_i}V_{i,\theta}\right] - (\xi+\nu_e)V_{e,r} - \frac{eB}{m_e}V_{e,\theta} + \frac{2\mu}{r}\right\} \tag{A4}$$

It is seen from Eq. (A4) that when

$$\mu[u_0{}^2 - V_{i,r}{}^2] - V_{e,r}{}^2 = 0 \tag{A5}$$

a critical point exists. Assuming that a critical point corresponds to a sheath edge, one finds from Eqs. (8) and (A5) that at the edge of the cathode sheath, $r = c$,

$$V_{i,r} = -[1/(1+\mu)]\{(j/2\pi cen) + [\mu(1+\mu)u_0{}^2 - \mu(j/2\pi cen)^2]^{1/2}\} \tag{A6}$$

Because the distance between the edge of the cathode sheath and that of the anode sheath is not known a priori when the complete equations, i.e., (A1–A3) are employed, Eqs. (8) and (A5) cannot be used to provide a boundary condition at the anode sheath. It is seen from Eq. (A6) that when $j = 0$

$$V_{i,r} = u_0 \tag{A7}$$

which is the isothermal speed of sound of the ion-electron pair.

Appendix B: General Dispersion Relation

Because of the nature of the steady-state solution, the functions $f(R)$ and $h(R)$ are assumed to have the representation

$$f(R) = 2\sum_{p=1}^{\infty}\frac{F_m(\delta_p)}{\gamma_{m,p}}G_m(\delta_pR) \tag{B1}$$

$$h(R) = 2\sum_{p=1}^{\infty}\frac{H_m(\delta_p)}{\gamma_{m,p}}G_m(\delta_pR) \tag{B2}$$

where

$$G_m(\delta_pR) = Y_m(\delta_pR)J_m(\delta_pc/a) - Y_m(\delta_pc/a)J_m(\delta_pR) \tag{B3}$$

and δ_p is a root of the equation

$$G_m(\delta_p) = 0 \tag{B4}$$

It can be shown by direct integration that the functions $G_m(\delta_jR)$ are orthogonal and

$$\int_{c/a}^{1} RG_m{}^2(\delta_jR)dR = \gamma_{m,j} \tag{B5}$$

where

$$\gamma_{m,j} = Q_{m-1}{}^2(\delta_j) - (c/a)^2Q_{m-1}{}^2(\delta_jc/a)$$
$$Q_{m-1}(\delta_jR) = Y_{m-1}(\delta_jR)J_m(\delta_jc/a) - J_{m-1}(\delta_jR)Y_m(\delta_jc/a) \tag{B6}$$

As is seen from Eqs. (B1) and (B2) and the properties of $G_m(\delta_j R)$, $F_m(\delta_p)$ and $H_m(\delta_p)$ are the integral transforms of $f(R)$ and $h(R)$, i.e.,

$$F_m(\delta_p) = \int_{c/a}^{1} Rf(R)G_m(\delta_p R)dR$$
$$H_m(\delta_p) = \int_{c/a}^{1} Rh(R)G_m(\delta_p)dR \tag{B7}$$

Also, the choice of $f(R)$ and $h(R)$ indicated in Eqs. (B1) and (B2) implies that the density and potential perturbations vanish at the edges of the cathode and anode sheaths.

Multiplying Eq. (24) by $RG_m(\delta_j R)$ and integrating, one obtains

$$\left[1 - \frac{\delta_j^2}{\beta_0^2} - i\omega_0 - \frac{k_0^2}{\beta_0^2}(1 + \mu_{i,e}^2 B^2)\right] F_m(\delta_j) \pm \frac{\mu'_{i,e}}{\xi a^2(\mu'_i + \mu'_e)}\left[m(1 \mp i\mu_{i,e}B)\sum_{p=1}^{\infty} a_{pj}F_m(\delta_p) - \delta_j \sum_{p=1}^{\infty} b_{pj}F_m(\delta_p)\right] = \pm \frac{\mu'_{i,e}}{a^2\xi}\left\{[\delta_j^2 + k_0^2(1 + \mu_{i,e}^2 B^2)] \times H_m(\delta_j) + m(1 \mp iB\mu_{i,e})\sum_{p=1}^{\infty} c_{pj}H_m(\delta_p) - \delta_j \sum_{p=1}^{\infty} d_{pj}H_m(\delta_p)\right\} \tag{B8}$$

where

$$a_{pj} = \frac{2}{\gamma_{m,p}}\int_{c/a}^{1} \frac{G_m(\delta_p R)G_m(\delta_j R)}{RN_0}\,dR$$
$$b_{pj} = \frac{2}{\gamma_{m,p}}\int_{c/a}^{1} \frac{G_m(\delta_p R)Q_{m-1}(\delta_j R)}{N_0}\,dR \tag{B9}$$
$$c_{pj} = \frac{2}{\gamma_{m,p}}\int_{c/a}^{1} G_m(\delta_p R)G_m(\delta_j R)\left(\frac{1}{N_0}\frac{dN_0}{dR}\right)dR$$
$$d_{pj} = \frac{2}{\gamma_{m,p}}\int_{c/a}^{1} RG_m(\delta_p R)Q_{m-1}(\delta_j R)\left(\frac{1}{N_0}\frac{dN_0}{dR}\right)dR$$

The dispersion relation is obtained by setting the determinant of the infinite system of equations represented by Eq. (B8) to zero. It is seen that the approximate dispersion relation given by Eq. (28) can be obtained from Eq. (B8)by letting $p = j = 1$.

References

[1] Ekdahl, C., Kribel, R., and Lovberg, R., "Internal Measurements of Plasma Rotation in an MPD Arc," AIAA Paper 67-655, Colorado Springs, Colo., 1967.

[2] Brockman, P. et al., "The Effect of Various Propellants and Propellant Mixtures on an MPD Arc Jet," AIAA Paper 67-684, Colorado Springs, Colo., 1967.

[3] Connolly, D. J. et al., "Low Environmental Pressure MPD Arc Tests," *AIAA Journal*, Vol. 6, No. 7, July 1968, pp. 1271–1276.

[4] Larson, A. V., "Experiments on Current Rotations in an MPD Engine," AIAA Paper 67-689, Colorado Springs, Colo., 1967.

[5] Sidney, B. D., Hess, R. V., and Allario, F., "Onset and Suppression of Plasma Instability in Crossed-Field Geometry," *Bulletin of the American Physical Society*, Vol. 13, No. 6, June 1968, p. 889.

[6] Malliaris, A. C., "Oscillations in an MPD Accelerator," *AIAA Journal*, Vol. 6, No. 8, Aug. 1968, pp. 1575–1577.

[7] Johnson, R. R. and Jerde, D. A., "Instability of a Plasma Column in a Longitudinal Magnetic Field," *The Physics of Fluids*, Vol. 5, No. 8, Aug. 1962, pp. 988–993.

[8] Garrison, G. W., Jr. and Hassan, H. A., "Screw Instability in a Linear Hall Accelerator," *The Physics of Fluids*, Vol. 10, No. 4, April 1967, pp. 711–718.

[9] Hoh, F. C., "Instability of a Penning-Type Discharge," *The Physics of Fluids*, Vol. 6, No. 8, Aug. 1963, pp. 1184–1191.

[10] Persson, K.-B., "Inertia-Controlled Ambipolar Diffusion," *The Physics of Fluids*, Vol. 5, No. 12, Dec. 1962, pp. 1625–1632.

[11] Simon, A., "Instability of a Partially Ionized Plasma in Crossed Electric and Magnetic Fields," *The Physics of Fluids*, Vol. 6, No. 3, March 1963, pp. 382–388.

[12] Seals, R. K., Jr. and Hassan, H. A., "Analysis of MPD Arcs with Nonequilibrium Ionization," *AIAA Journal*, Vol. 6, No. 12, Dec. 1968, pp. 2273–2278.